CRIMSON PUBLISHERS
Wings to the Research

Research & Development in Material Science

ISSN: 2576-8840

Research Article

Influence of Titanium Oxide on Structure, Corrosion and Soldering Properties of $Sn_{82}Bi_{15}Zn_3$ Alloy

Abu Bakr El-Bediwi* and Reham Samir

Department of Physics, Egypt

***Corresponding author:** Abu Bakr El-Bediwi, Department of Physics, Metal Physics Lab, Faculty of Science, Egypt,

Submission: March 28, 2018; **Published:** May 14, 2018

Abstract

Our work study the effect of titanium oxide on structure, soldering properties such as melting temperature, wetting process and corrosion behavior of $Sn_{82}Bi_{15}Zn_3$ alloy. Microstructure of $Sn_{82}Bi_{15}Zn_3$ alloy changed after adding different ratio from titanium oxide. Lattice microstrain of $Sn_{82}Bi_{15}Zn_3$ alloy varied (increased) after adding titanium oxide. Melting temperature of $Sn_{82}Bi_{15}Zn_3$ alloy varied after adding Ti2O. $Sn_{81.4}Bi_{15}Zn_3(Ti_2O)_{0.6}$ alloy has low melting temperature. The contact angle $Sn_{82}Bi_{15}Zn_3$ alloy decreased after adding different ratio from titanium oxide. Corrosion resistance of $Sn_{82}Bi_{15}Zn_3$ alloy varied (increased) after adding Ti_2O. From our results, soldering properties (melting temperature and contact angle) and corrosion resistance of $Sn_{82}Bi_{15}Zn_3$ alloy improved after adding Ti_2O.

Keywords: High tin alloy; Ti_2O; Corrosion; Contact angle; Melting temperature

Introduction

Soldering is a low temperature metallurgical joining process. In electronics applications low temperature and reversibility are especially important because of the materials involved and the necessity for reworking and making engineering changes. Solder joining is a wetting process followed by a chemical reaction. Wettability is a function of the materials to be joined, with Cu, Ni, Au, and Pd, as well as alloys rich in one or more of these metals, being particularly amenable to soldering. The chemical reaction following wetting is between the molten solder and the joining metallurgy to form an intermetallic phase region at the interface. Microstructure, wettability and physical properties of $Sn_{96-x}Zn_4Bi_x$ alloys are reported by El-Bediwi et al. [1]. The melting temperature of $Sn_{96}Zn_4$ alloy decreased after adding bismuth. But contact angle of $Sn_{96}Zn_4$ alloy varied after adding bismuth. Adding silver caused a significant increase in bismuth-tin-zinc alloy strengthens with a little decreased in melting temperature [2]. El-Bediwi et al. [2] reported that, there is a significant decrease in melting temperature of bismuth-tin-zinc alloy with a very little increase in strengthens after adding indium. Microstructure, thermal parameters, wettability and electrochemical corrosion process of $Bi_{30}Sn_{50}Sb_{10}A_{l5}Zn_3Cu_2$, $Bi_{25}Sn_{61}Sb_5Zn_4Al_3Ag_2$, and $Bi_{20}Sn_{60}Sb_7A_{l5}Zn_3Cd_3Cu_2$, alloys have been studied [3]. Microstructure, wettability behavior, corrosion parameters, thermal properties of quaternary bismuth- tin based alloy have been investigated using different experimental techniques and the results show that, some properties of $Bi_{60}Sn_{40}$ alloy improved after adding Sb-Zn or Sb-Ag elements [4]. Tin- zinc eutectic alloy has been considered as a candidate for lead free solder materials because of its low melting point, excellent mechanical properties and low cost [5-7]. Mostly solders are based on Sn-containing binary and ternary alloys. Several elements have been selected as alloying elements such as Zn, Bi, Cu, Ag, Sb and so on [8-10]. Specific researchers [11-15] reported that, tin- zinc eutectic solder alloy is poor wettability, reliability, strength, easy oxidation and microvoid formation. To avoid these disadvantages or improve the properties of it, they added minor amount of Bi, Cu, In, Ag, Al, Ga, Sb, Cr, Ni, Ge elements to develop ternary and even quaternary Pb free alloys. The aim of our work was to study the effect of titanium dioxide on microstructure, soldering properties and corrosion of tin bismuth-zinc alloy.

Materials and Methods

High purity (tin, bismuth and zinc) metal and titanium dioxide (white color) are used to prepare $Sn_{82}Bi_{15}Zn_3(Ti_2O)_x$ (x=0,0.3,0.6,0.9 and 1.2) alloys. These alloys (mixed metals and Ti_2O by weight percentage) are melted then normal casted on substrate in air. The samples from alloys are prepared in convenient shape for all tests such as microstructure, thermal parameters, wettability and

corrosion behavior. Microstructure of used alloys was performed using Shimadzu X-ray Diffractometer, (Dx-30, Japan) Cu–Ka radiation with l=1.54056 Å at 45kV and 35mA and Ni–filter, in the angular range 2q ranging from 0 to 100° in continuous mode with a scan speed 5deg/min and scanning electron microscope (JEOL JSM-6510LV, Japan). The polarization studies were performed using Gamry Potentiostat/Galvanostat with a Gamry framework system based on ESA 300. Gamry applications include software DC105 for corrosion measurements and Echem Analyst version 5.5 software packages for data fitting. The differential scanning calorimetry (DSC) thermographs were obtained by Universal V4. 5A TA instrument with heating rate 10k/min in the temperature range 0-400 °C.

Results and Discussion

X- ray diffraction analysis

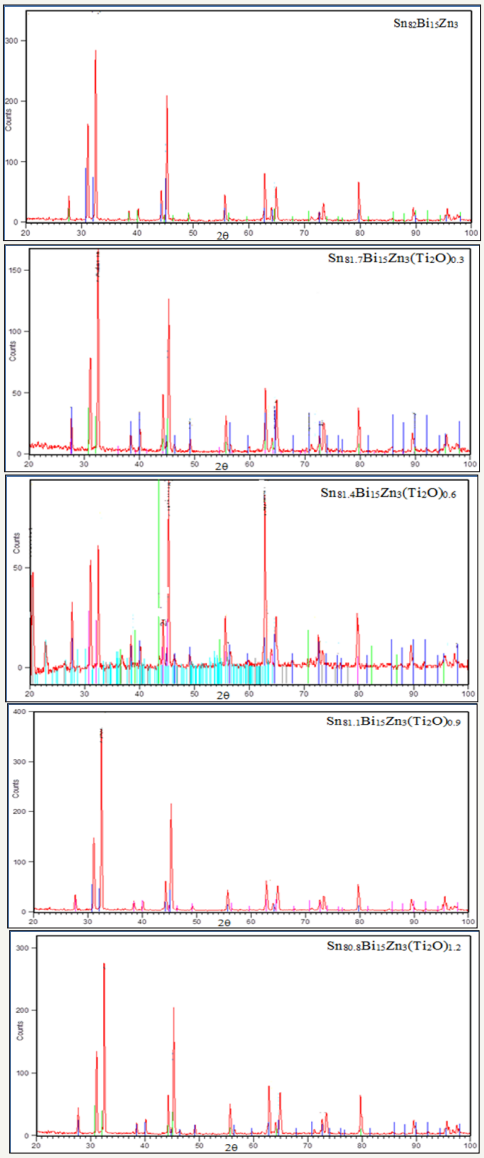

Figure 1: x-ray diffraction patterns of $Sn_{82-x}Bi_{15}Zn_3(Ti_2O)_x$ alloys.

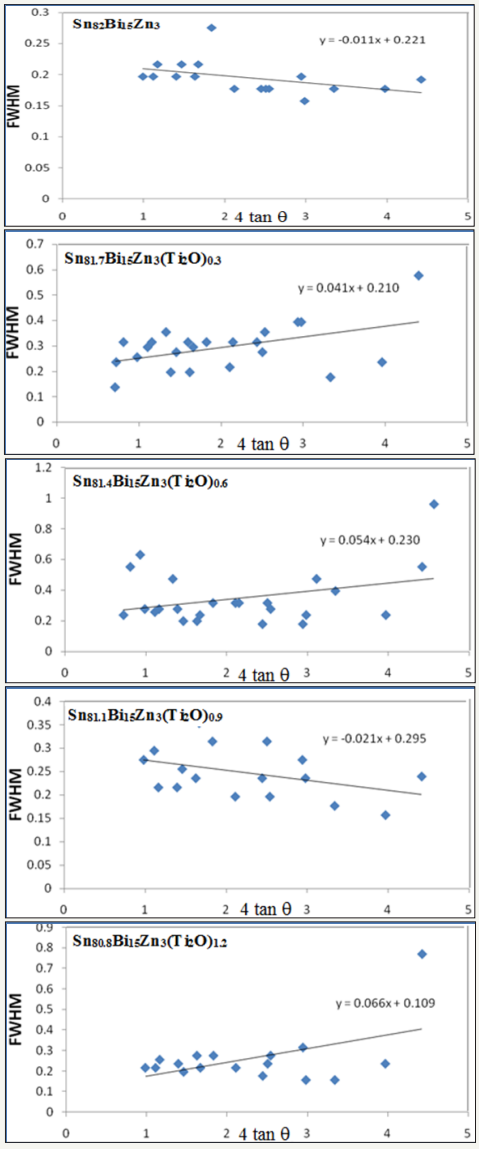

Figure 2: FWHM versus 4tanθ for $Sn_{82-x}Bi_{15}Zn_3(Ti_2O)_x$ alloys. alloys.

Table 1: x-ray diffraction patterns of $Sn_{82-x}Bi_{15}Zn_3(Ti_2O)_x$alloys.

$Sn_{81.7}Bi_{15}Zn_3(Ti_2O)_{0.3}$ Alloy						
2θ	d Å	Int. %	Phase	hkl	FWHM	Area
20.1708	4.40243	18.7	Bi	003	0.1378	4.5
20.5734	4.31719	27.91	Bi	003	0.2362	11.5
23.008	3.86558	10.11	Bi	012	0.3149	5.56
27.5571	3.23692	38.35	Bi	012	0.2558	17.12
30.9694	2.88761	98.21	Sn	200	0.2952	50.59
32.3271	2.76937	100	Sn	101	0.3149	54.95
36.834	2.44021	4.07	Zn	002	0.3542	2.52
38.3222	2.3488	11.32	Bi	104	0.1968	3.89
40.0254	2.2527	11.27	Bi	110	0.2755	5.42
43.5884	2.07646	5.37	Sn	220	0.3149	2.95

44.1079	2.05321	29.44	Bi	015	0.1968	10.11
45.1593	2.00782	71.92	Sn	211	0.2952	37.05
49.0546	1.85711	6.03	Bi	202	0.3149	3.32
55.5567	1.65418	15.86	Sn	301	0.2165	5.99
56.4327	1.63057	4.81	Bi	024	0.3149	2.64
62.7327	1.48112	24.21	Sn	112	0.3149	13.3
64.1149	1.45249	11.48	Sn	400	0.2755	5.52
64.7323	1.44012	17.05	Sn	321	0.3542	10.54
72.5751	1.30261	7.75	Sn	321	0.3936	5.32
73.3377	1.29094	11.46	Sn	411	0.3936	7.87
79.6088	1.20427	19.58	Sn	312	0.1771	6.05
89.4527	1.09551	9.83	Bi	306	0.2362	4.05
95.5354	1.04035	6.66	Sn	431	0.576	9.05

$Sn_{81.4}Bi_{15}Zn_3(Ti_2O)_{0.6}$ Alloy						
2θ	d Å	Int. %	Phase	hkl	FWHM	Area
20.4931	4.33393	51.5	Bi	003	0.2362	11.13
22.7914	3.90183	12.71	Bi	003	0.551	6.41
27.6874	3.22199	33.89	Bi	012	0.2755	8.54
31.0357	2.88159	57.73	Sn	200	0.2558	13.51
32.4191	2.76172	65.81	Sn	101	0.2755	16.59
36.8433	2.43961	5.57	Zn	002	0.4723	2.41
38.3326	2.34819	13.12	Bi	104	0.2755	3.31
40.1666	2.2451	11.11	Bi	110	0.1968	2
44.3916	2.04074	16.54	Bi	015	0.1968	2.98
45.2717	2.0031	100	Sn	211	0.2362	21.61
49.1533	1.85361	7.46	Bi	202	0.3149	2.15
55.5652	1.65395	22.25	Sn	301	0.3149	6.41
56.5443	1.62762	6.68	Bi	024	0.3149	1.92
62.8005	1.47969	82.81	Sn	112	0.1771	13.42
64.075	1.4533	8.01	Sn	400	0.3149	2.31
64.8742	1.43731	26.45	Sn	321	0.2755	6.67
72.641	1.3016	16.2	Sn	321	0.1771	2.63
73.4118	1.28982	7.5	Sn	411	0.2362	1.62
75.7304	1.25599	2.52	Bi	125	0.4723	1.09
79.7846	1.20206	25.26	Sn	312	0.3936	9.1
89.5289	1.09478	11.87	Bi	306	0.2362	2.56
95.6638	1.04015	5.71	Sn	431	0.551	2.88
97.5263	1.02435	4.74	Bi	134	0.96	5.63

$Sn_{81.1}Bi_{15}Zn_3(Ti_2O)_{0.9}$ Alloy						
2θ	d Å	Int. %	Phase	hkl	FWHM	Area
27.5918	3.23293	8.4	Bi	012	0.2755	8.18
31.074	2.87813	39.92	Sn	200	0.2952	41.66
32.4508	2.75909	100	Sn	101	0.2165	76.54
38.4239	2.34282	4.76	Bi	104	0.2165	3.65
40.0563	2.25103	4.77	Bi	110	0.2558	4.31
44.228	2.04791	15.01	Bi	015	0.2362	12.53
45.2447	2.00423	56.03	Sn	211	0.3542	70.18
49.202	1.8519	3.11	Bi	202	0.3149	3.46
55.6714	1.65105	11.29	Sn	301	0.1968	7.86
62.86	1.47843	16.21	Sn	112	0.2362	13.54
64.0876	1.45304	3.63	Sn	400	0.3149	4.04
64.7986	1.43881	9.62	Sn	321	0.1968	6.69
72.643	1.30156	5.51	Sn	321	0.2755	5.36
73.3404	1.2909	6.98	Sn	411	0.2362	5.83
79.7009	1.20311	14.52	Sn	312	0.1771	9.09
89.518	1.09488	6.05	Bi	306	0.1574	3.37
95.6174	1.03967	6.82	Sn	431	0.24	7.82

Sn80.8Bi15Zn3(Ti2O)1.2 Alloy						
2θ	d Å	Int. %	Phase	hkl	FWHM	Area
27.6769	3.22318	15.21	Bi	012	0.2165	8.85
31.0759	2.87796	48.2	Sn	200	0.2165	28.03
32.4585	2.75845	100	Sn	101	0.2558	68.74
38.4607	2.34066	6.48	Bi	104	0.2362	4.11
40.1365	2.24672	8.94	Bi	110	0.1968	4.73
44.2714	2.046	22.76	Bi	015	0.2755	16.85
45.2937	2.00218	74.14	Sn	211	0.2165	43.13
49.2117	1.85155	5.81	Bi	202	0.2755	4.3
55.6382	1.65196	15.95	Sn	301	0.2165	9.28
62.8665	1.47829	27.61	Sn	112	0.1771	13.14
64.1401	1.45198	5.96	Sn	400	0.2362	3.78
64.88	1.4372	23.46	Sn	321	0.2755	17.37
72.7066	1.30058	7.03	Sn	321	0.3149	5.95
73.4005	1.28999	11.92	Sn	411	0.1574	5.04
79.7325	1.20271	22.66	Sn	312	0.1574	9.58
89.5495	1.09458	7.89	Bi	306	0.2362	5.01
95.7834	1.03831	4.12	Sn	431	0.768	11.48

Table 2: Lattice microstrain of $Sn_{82-x}Bi_{15}Zn_3(Ti_2O)_x$ alloys.

Alloys	e
$Sn_{82}Bi_{15}Zn_3$	0.011
$Sn_{81.7}Bi_{15}Zn_3(Ti_2O)_{0.3}$	0.041
$Sn_{81.4}Bi_{15}Zn_3(Ti_2O)_{0.6}$	0.054
$Sn_{81.1}Bi_{15}Zn_3(Ti_2O)_{0.9}$	0.021
$Sn_{80.8}Bi_{15}Zn_3(Ti_2O)_{1.2}$	0.066

X-ray diffraction patterns, Figure 1, of $Sn_{82}Bi_{15}Zn_3(Ti_2O)_x$ (x=0.3,0.6,0.9 and 1.2) alloys have lines corresponding to tetragonal β-Sn phase, hexagonal Bi phase, Zn phase with undetected Ti_2O or intermetallic compounds and solid solution from dissolved atoms changed its matrix structure. The details of x-ray analysis such as the peak intensity (crystallinity), peak broadness (crystal size) and peak position (orientation) of $Sn_{82}Bi_{15}Zn_3$ alloy changed after adding different ratio of titanium dioxide as listed in Table 1. That is because Ti_2O nanoparticles formed undetected intermetallic compounds with dissolved atoms in matrix alloy. Lattice microstrain, ε, which

How to cite this article: Abu B E-B, Reham S. Influence of Titanium Oxide on Structure, Corrosion and Soldering Properties of $Sn_{82}Bi_{15}Zn_3$ Alloy . Res Dev Material Sci . 6(1). RDMS.000630.2018. DOI: 10.31031/RDMS.2018.06.000630

determined from the relation between full width half maximum, FWHM, and 4tanθ using Williamson and Hall equation [15] is presented in Figure 2. Lattice microstrain of $Sn_{82}Bi_{15}Zn_3$ alloy varied (increased) after adding titanium dioxide as listed in Table 2.

Scanning electron microscope analysis (SEMA)

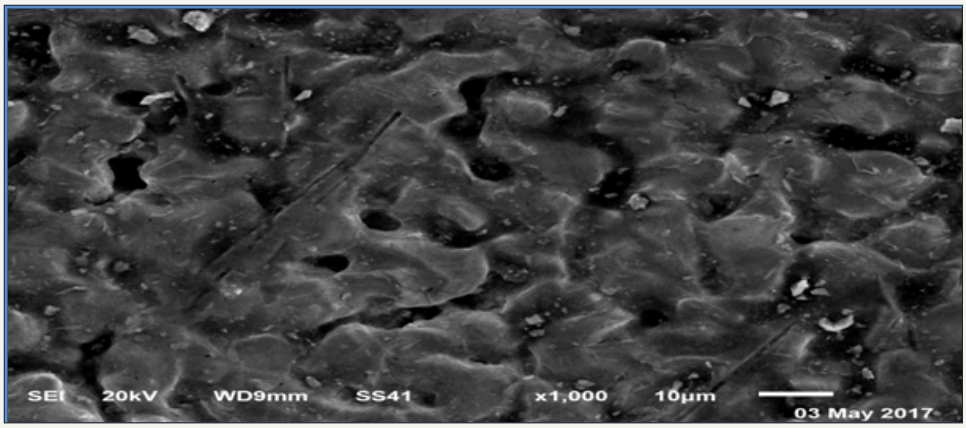

Figure 3a: SEM of $Sn_{82}Bi_{15}Zn_3$ alloy.

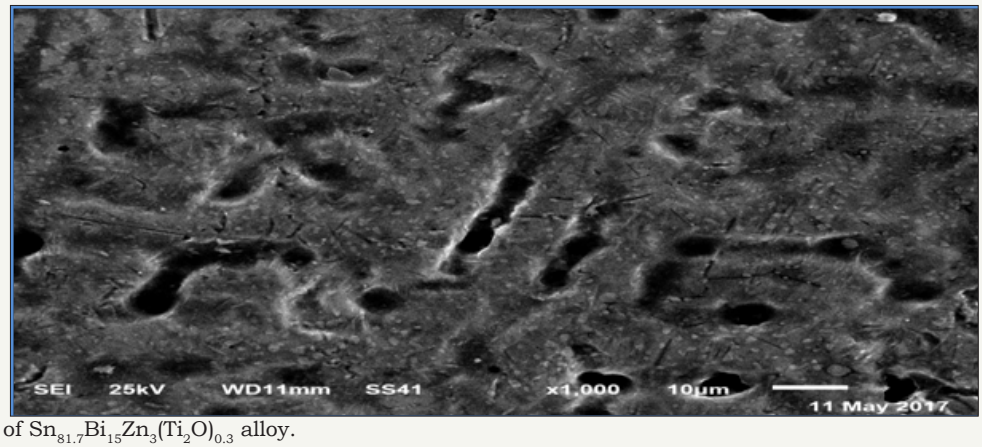

Figure 3b: SEM of $Sn_{81.7}Bi_{15}Zn_3(Ti_2O)_{0.3}$ alloy.

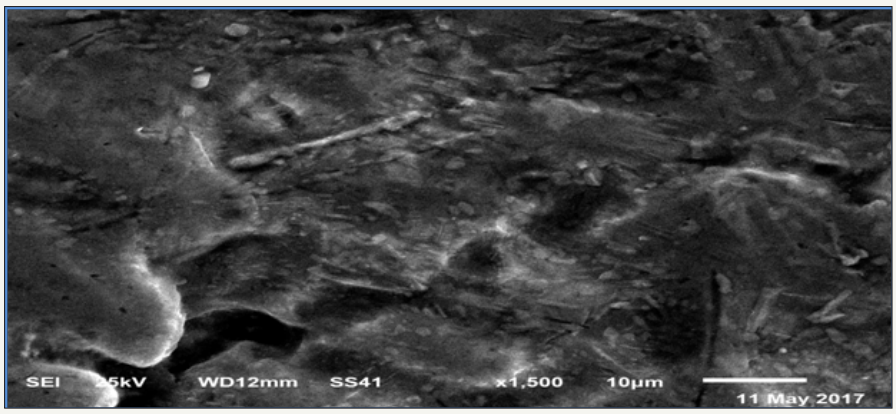

Figure 3c: SEM of $Sn_{81.4}Bi_{15}Zn_3(Ti_2O)_{0.6}$ alloy.

Scanning electron micrographs (SEM) of $Sn_{82}Bi_{15}Zn_3(Ti_2O)_x$ (x=0,0.3,0.6,0.9 and 1.2) are shown in Figure 3a-3e. SEM of $Sn_{82}Bi_{15}Zn_3$ alloy has lamellar structure (tin phase is a gray color, bismuth phase is a black color) contained white color (which is zinc or bismuth-tin or cluster from dissolved atoms) with different shape and size. $Sn_{81.7}Bi_{15}Zn_3(Ti_2O)_{0.3}$ alloy has homogenous structure from tin phase (gray color), slabs and spherical shape from bismuth phase (black color) and little spherical grain or around slab from undetected phases (white\or gray) such as zinc or Ti_2O or intermetallic phases. $Sn_{81.4}Bi_{15}Zn_3(Ti_2O)_{0.6}$ alloy has heterogeneous structure formed from tin phase as a gray color contained bismuth phase as black color and little spherical with slab at grain boundary of undetected phases (zinc or Ti_2O or intermetallic phases) as gray/ or white color. $Sn_{81.1}Bi_{15}Zn_3(Ti_2O)_{0.9}$ alloy has heterogeneous matrix structure (slabs and spherical with different size\ orientation) as gray color contained lamellar structure bismuth phase as black

How to cite this article: Abu B E-B, Reham S. Influence of Titanium Oxide on Structure, Corrosion and Soldering Properties of $Sn_{82}Bi_{15}Zn_3$ Alloy . Res Dev Material Sci . 6(1). RDMS.000630.2018. DOI: 10.31031/RDMS.2018.06.000630

color and undetected phases (spherical/ around grains) as gray or white color. $Sn_{80.8}Bi_{15}Zn_3(Ti_2O)_{1.2}$ alloy has heterogeneous matrix structure of tin phase (gray color) contained spherical bismuth phase (black color) surround by white\or gray color as zinc or Ti_2O or intermetallic phases. From SEMA, adding Ti_2O to $Sn_{82}Bi_{15}Zn_3$ alloy caused a change in its matrix microstructure (quantity, size and orientation of formed phases).

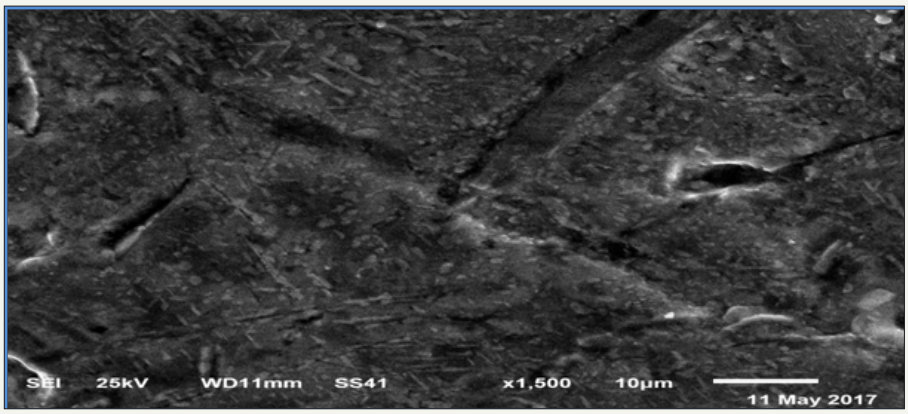

Figure 3d: SEM of $Sn_{81.1}Bi_{15}Zn_3(Ti_2O)_{0.9}$ alloy.

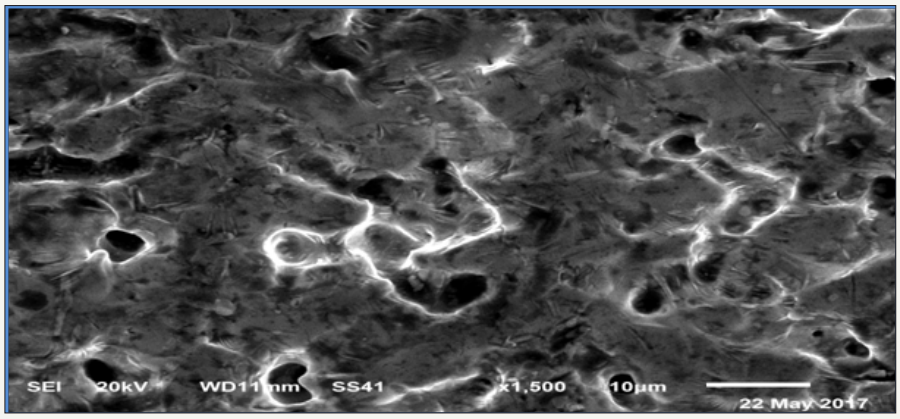

Figure 3e: SEM of $Sn_{80.8}Bi_{15}Zn_3(Ti_2O)_{1.2}$ alloy.

Solder properties

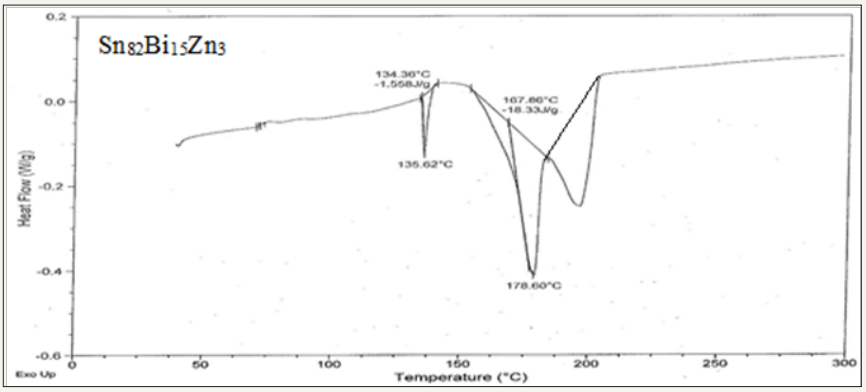

Figure 4a: DSC graph of $Sn_{82}Bi_{15}Zn_3$ alloy.

Solder alloys are characterized by the melting temperature being a strong function of composition. Differenitional scanning calometric graphs of $Sn_{82}Bi_{15}Zn_3(Ti_2O)_x$ (x=0,0.3,0.6,0.9 and 1.2) alloys which have more peaks (related more phases) are shown in Figure 4a-4e. Adding titanium dioxide caused a change in DSC shape, intensity and broadness of $Sn_{82}Bi_{15}Zn_3$ alloy like x-ray diffraction patterns. That is because Ti_2O changed matrix alloy microstructure such as formed phases and atoms dissolved formed a cluster of atoms or solid solution. Melting temperature of $Sn_{82}Bi_{15}Zn_3$ alloy varied after adding Ti_2O as listed in Table 3. $Sn_{81.4}Bi_{15}Zn_3(Ti_2O)0.6$ alloy has low melting temperature.

How to cite this article: Abu B E-B, Reham S. Influence of Titanium Oxide on Structure, Corrosion and Soldering Properties of $Sn_{82}Bi_{15}Zn_3$ Alloy . Res Dev Material Sci . 6(1). RDMS.000630.2018. DOI: 10.31031/RDMS.2018.06.000630

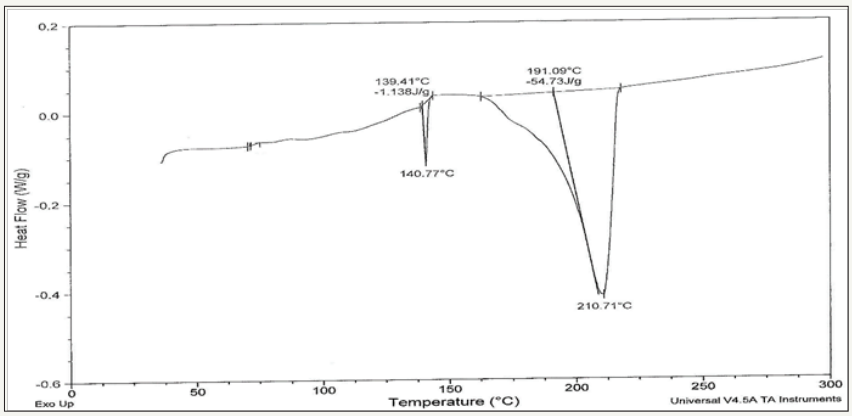

Figure 4b: DSC graph of $Sn_{81.7}Bi_{15}Zn_3(Ti_2O)_{0.3}$ alloy.

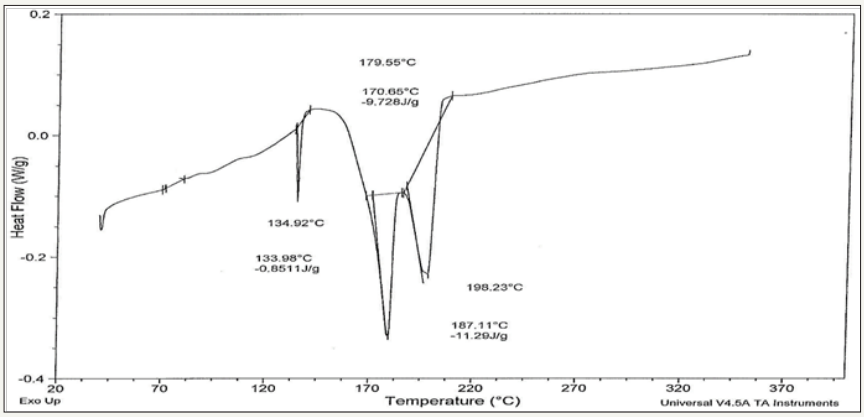

Figure 4c: DSC graph of $Sn_{81.4}Bi_{15}Zn_3(Ti_2O)_{0.6}$ alloy.

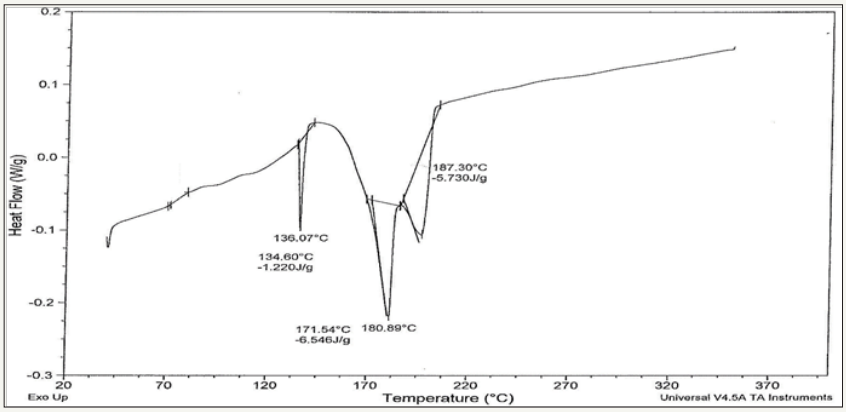

Figure 4d: DSC graph of $Sn_{81.1}Bi_{15}Zn_3(Ti_2O)_{0.9}$ alloy.

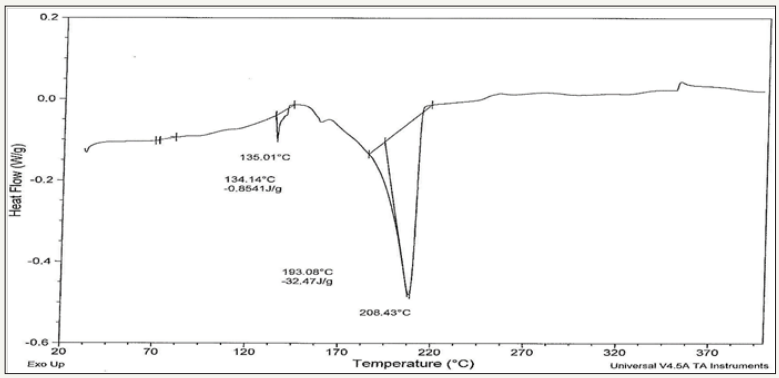

Figure 4e: DSC graph of $Sn_{80.8}Bi_{15}Zn_3(Ti_2O)_{1.2}$ alloy.

Table 3: Melting temperature of $Sn_{82-x}Bi_{15}Zn_3(Ti_2O)_x$ alloys.

Alloys	Melting Temperature °C
$Sn_{96}Zn^4$	216.42
$Sn_{82}Bi_{15}Zn_3$	212
$Sn_{81.7}Bi_{15}Zn_3(Ti_2O)_{0.3}$	210.7
$Sn_{81.4}Bi_{15}Zn_3(Ti_2O)_{0.6}$	187.11
$Sn_{81.1}Bi_{15}Zn_3(Ti_2O)_{0.9}$	187.3
$Sn_{80.8}Bi_{15}Zn_3(Ti_2O)_{1.2}$	208.43

The contact angle $Sn_{82}Bi_{15}Zn_3$ alloy decreased after adding different ratio from titanium dioxide as presented in Table 4. That is meant, the spreading of molten $Sn_{82}Bi_{15}Zn_3$ alloy increased in copper surface substrate.

Table 4: Contact angles of $Sn_{82-x}Bi_{15}Zn_3(Ti_2O)_x$ alloys

Alloys	Contact Angle
$Sn_{82}Bi_{15}Zn_3$	21.25±2
$Sn_{81.7}Bi_{15}Zn_3(Ti_2O)_{0.3}$	19.5±1.5
$Sn_{81.4}Bi_{15}Zn_3(Ti_2O)_{0.6}$	19.25±1.5
$Sn_{81.1}Bi_{15}Zn_3(Ti_2O)_{0.9}$	17.75±1.25
$Sn_{80.8}Bi_{15}Zn_3(Ti_2O)_{1.2}$	15.5±1

Corrosion behavior

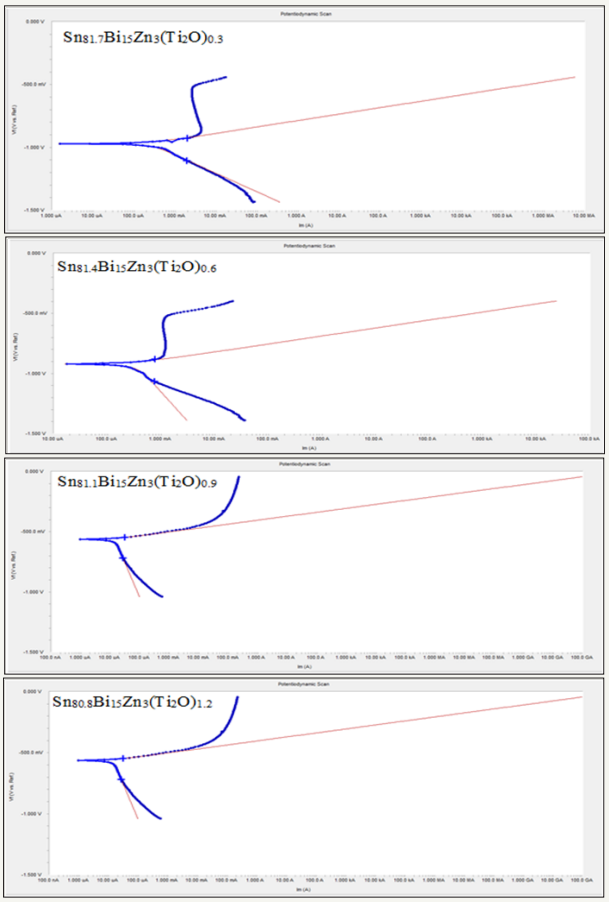

Figure 5: Electrochemical polarization curves of $Sn_{82-x}Bi_{15}Zn_3(Ti_2O)_x$ alloys.

Electrochemical polarization curves of $Sn_{82}Bi_{15}Zn_3(Ti_2O)_x$ (x=0.3,0.6,0.9 and 1.2) alloys in 0.25M HCl are shown in Figure 5. They show, the corrosion potential of used alloys exhibited a negative potential. Also the cathodic and the anodic polarization curves showed similar corrosion trends. The corrosion potential (E_{Corr}), corrosion current (I_{Corr}) and corrosion rate ($Corr_{Rate}$) of $Sn_{82}Bi_{15}Zn_3Ti_2O_x$ alloys are presented in Table 5. Corrosion rate and corrosion current of $Sn_{82}Bi_{15}Zn_3$ alloy decreased (varied) after adding Ti_2O. That is because adding different ratio of Ti_2O caused formed new phases and cluster of atoms or solid solution which effects on atoms segregation and their reactivity with HCl. We recommended to study the effect of Ti_2O from 0.1 to 0.9 with 0.1 step.

Table 5: Corrosion parameters of $Sn_{82-x}Bi_{15}Zn_3(Ti_2O)_x$ alloys.

Alloys	E_{corr} (mV)	I_{corr} (uA)	$Corr_{Rate}$ (mpy)
$Sn_{82}Bi_{15}Zn_3$	-862	841	348.3
$Sn_{81.7}Bi_{15}Zn_3(Ti_2O)_{0.3}$	-554	515	235.4
$Sn_{81.4}Bi_{15}Zn_3(Ti_2O)_{0.6}$	-970	249	113.8
$Sn_{81.1}Bi_{15}Zn_3(Ti_2O)_{0.9}$	-919	336	153.5
$Sn_{80.8}Bi_{15}Zn_3(Ti_2O)_{1.2}$	-563	342	164.67

Conclusion

1. Adding Ti_2O to $Sn_{82}Bi_{15}Zn_3$ alloy caused a change in its matrix microstructure (crystallinity, size and orientation of formed phases in matrix).
2. Lattice microstrain of $Sn_{82}Bi_{15}Zn_3$ alloy varied (increased) after adding titanium dioxide.
3. Melting temperature of $Sn_{82}Bi_{15}Zn_3$ alloy varied (decreased) after adding Ti_2O.
4. The contact angle $Sn_{82}Bi_{15}Zn_3$ alloy decreased after adding different ratio from titanium dioxide.
5. Corrosion rate of $Sn_{82}Bi_{15}Zn_3$ alloy decreased (varied) after adding Ti_2O.
6. Soldering properties such as melting temperature and spreading (contact angle) of $Sn_{82}Bi_{15}Zn_3$ alloy improved and very closed to lead- tin commercial solder alloy (M.P=183 °C and contact angle ~ 19°) after adding Ti_2O.
7. Corrosion resistance of $Sn_{82}Bi_{15}Zn_3$ alloy also is improved by adding $T_{i2}O$.

References

1. El-Bediwi AB, El-Shafei A, Kamal M (2015) Microstructure, physical and soldering properties of Tin-Zinc-Bismuth alloy. MSAIJ 12(2): 2-28.
2. El-Bediwi AB, Dawood F, Kamal M (2015) Effect of quaternary addition on structure, electrical, mechanical and thermal properties of bismuth-tin-zinc rapidly solidified fusible alloy. Journal of Advances in Physics 7(3): 1952-1958.

3. El-Bediwi AB, Bader S, Khalifa F (2016) Microstructure, electrochemical corrosion behavior and soldering properties of hexa and hepta bismuth-tin based alloy. Global Journal of Physics 4(3): 480-495.

4. El-Bediwi AB, Bader S, Khalifa F (2016) Effect of Alloying Elements on Electrochemical Corrosion Behavior, Microstructure, Wettability and Thermal Performance of Bismuth-Tin Based Alloys. IJSRSET 2(2): 1267-1277.

5. Yang W, Messler RW (1994) Microstructure evolution of eutectic Sn-Ag solder joints. J Electron Mater 23(8): 765-772.

6. Mavoori H, Chin J, Vaynman S (1997) J Electron Mater 41: 1269.

7. McCormack M, Jin S, Kammlott DGW (1995) Proceedings of the 1995 IEEE international symposium on electronics and the environment, ISEE, Orlando, FL, USA, pp. 1-3 171.

8. Abtew M, Selvaduray G (2000) Lead-free solders in microelectronics. Mater Sci Eng Rep 27(5-6): 95-141.

9. Vincent JH, Humpston G (1994) GEC J Res 11: 76.

10. Harrison MR, Vincent JH, Steen HAH (2001) Sold Surf Mount Technol 13: 21.

11. Kim KS, Yang JM, Yu CH, Jung IO, Kim HH (2004) Analysis on interfacial reactions between Sn-Zn solders and the Au/Ni electrolytic-plated Cu pad. J Alloy Compd 379: 314.

12. Anderson IE, Foley JC, Cook BA, Harringa J, Terpstra RL, et al. (2001) J Electron Mater 30(9): 1050.

13. McCormack M, Jin S, Kammlott GW, Chen HS (1993) New Pb-free solder alloy with superior mechanical properties. Appl Phys Lett 63(15).

14. Miric AZ, Grusd A (1998) Lead-free alloys. Surf Mount Technol 10(1): 1-19.

15. Williamson GK, Hall WH (1953) X-ray line broadening from filed aluminium and wolframL'elargissement des raies de rayons x obtenues des limailles d'aluminium et de tungsteneDie verbreiterung der roentgeninterferenzlinien von aluminium- und wolframspaenen. Acta Metallurgy 1(1): 22-31.